Plant Cell, Tissue and Organ Culture (2005) 81: 255–264
DOI 10.1007/s11240-004-6646-1

Application of bioreactor design principles to plant micropropagation

Wayne R. Curtis
*108 Fenske Laboratory, Department of Chemical Engineering, The Pennsylvania State University, University Park, PA 16802-4400, USA (*request for offprints: Fax: +1-814-865-7846; E-mail: wrc2@psu.edu)*

Key words: oxygen transport, respiration, somatic embryogenesis, suspension culture, tissue culture

Abstract

Principles of oxygen consumption, oxygen transport, suspension, and mixing are discussed in the context of propagating aggregates of plant tissue in liquid suspension bioreactors. Although micropropagated plants have a relatively low biological oxygen demand (BOD), the relatively large tissue size and localization of BOD in meristematic regions will typically result in oxygen mass transfer limitations in liquid culture. In contrast to the typical focus of bioreactor design on gas–liquid mass transfer, it is shown that media-solid mass transfer limitations limit oxygen available for aerobic plant tissue respiration. Approaches to improve oxygen availability through gas supplementation and bioreactor pressurization are discussed. The influence of media components on oxygen availability are also quantified for plant culture media. Experimental studies of polystyrene beads in suspension in a 30-l air-lift and stirred bioreactors are used to illustrate design principles for circulation and mixing. Potential limitations to the use of liquid suspension culture due to plant physiological requirements are acknowledged.

Introduction

Bioreactors for micropropagation cover a wide range of size (0.5–500 l) and complexity (jelly jar to modified microbial fermenter). The intention of this review is not to focus on (or promote) any particular bioreactor configuration, but to examine bioreactor design principles as they can be applied to the proliferation of micropropagules in bioreactor systems. This general approach is intended to provide some basis for considering alternative bioreactors for a specific culture system. Although simple tissue culture vessels are bioreactors, the focus of the principles presented here is on liquid-culture bioreactors. The associated analysis for submerged-culture propagation is on the typical limitations of oxygen transfer and mixing as they apply to micropropagules such as suspended somatic embryos.

Micropropagule oxygen demand

Analyzing the transport of oxygen in any bioreactor system is a characterization of oxygen gradients and the thermodynamic equilibria that determine the solubility of oxygen in media and plant tissue. The rate at which oxygen is consumed is a key determinant in these gradients. It is important to keep in mind that plant tissues in culture are predominantly – if not exclusively – growing heterotrophically on sugars. Fundamentally, this is no different to the heterotrophic utilization of sugars that takes place in all living tissues. Sugar oxidation therefore becomes a primary determinant of the tissue biological oxygen demand (BOD). Not only is the plant not producing oxygen *via* photosynthesis, but the typical limitations of carbohydrate synthesis and transport are not present. As a result, heterotrophic tissue culture can be expected to become kinetically limited by its biochemical capacity to

utilize nutrients. Surprisingly, the reported rates of oxygen consumption in suspensions are comparable to reports of plant respiration (Table 1). This suggests that other aspects of metabolism, such as the rate of utilization of energy derived from respiration, or transport inside the tissue might be rate-limiting for aerobic respiration.

The low solubility of oxygen in media is a fundamental limitation to oxygen use in biological systems. This can be illustrated using the average plant BOD of 10 μmol O_2 g^{-1} FW tissue. A tissue culture vessel containing 100 g FW tissue per litre would have sufficient oxygen for 8.5 h of respiration from air, but only 15 min if it contained water saturated with oxygen from air. The consequences of oxygen solubility on micropropagule development will be discussed in more detail in subsequent sections.

Oxygen transfer rate

The average BOD can also be used to carry out an initial 'ball park' estimate of oxygen transfer rates (OTR) needed to supply oxygen. Under balanced equilibrium conditions, total demand will be equal to the oxygen transfer rate from the gas to the media (OTR_{g-L}):

$$OTR_{g-L} = BOD \cdot \rho_t \cdot V_t = k_L a(C^* - C_L) \qquad (1)$$

Table 1. Oxygen uptake rates (OUR) of plant tissues and plant tissue culture

Plant	OUR[a]
Alfalfa (*Medicago sativa*, germinating seed, 18 °C)	44
Wheat (*Triticum aestivum*, seedling, 18 °C)	8.8
Corn (*Zea mays*, seedling, 18 °C)	6.3
Pea (*Pisum sativum*, seed, 20 °C)	6.2
Rye (*Secale cereale*, seedling, 18 °C)	5.0
Potato (*Solanum tuberosum*, whole plant, 19 °C)	4.5
Tobacco (*Nicotiana tabacum*, whole plant, 20 °C)	3.2
Plant tissue culture[b]	
Bulk tissue	10–12
Root meristem	200–300

[a] Data from compilation reference (Altman and Dittmer, 1968); μmol O_2 g^{-1} FW h l^{-1}.
[b] Average values from experimental measurements and quoted literature values.

where ρ_t is the tissue density (1.04 g ml^{-1}; approximately water), V_t is the tissue volume, C^* and C_L are the equilibrium and actual medium dissolved oxygen concentrations, and $k_L a$ is a parameter used to characterize the rate of oxygen transfer from the gas phase to the medium. To provide for diffusion of oxygen into the tissue it is reasonable to take $C_L \approx C^*/2$, therefore, an estimate for $k_L a$ of 8 h^{-1} can be calculated as the mass transfer rate needed to supply a typical plant tissue culture BOD. This initial calculation leads to a misleading conclusion, since this rate of oxygen transfer should be easy to achieve in just about any bioreactor configuration (simple shake flasks or blowing of bubbles in media would greatly exceed this level; Blanch and Clark, 1997). This apparent ease of supplying oxygen is qualitatively consistent with the observation that slow-growing plant tissues should have much lower oxygen demand than microbial cultures, none-the-less, experimentation has shown that plant tissues very often display oxygen-limited behavior. For example, the doubling of O_2 concentration in a flask headspace doubles the root extension rate and biomass accumulation rates in root culture (Asplund and Curtis, 2001).

There are several flaws in the preceding simplistic analysis of oxygen demand and oxygen transfer. An inherent assumption of the analysis is that oxygen demand is distributed evenly throughout the media. This is a reasonable assumption for microorganisms, but not for aggregates of plant tissue. Not only is the BOD not distributed throughout the bioreactor as for single cell suspensions, but the BOD is also distributed unevenly within the tissue. The oxygen demand at meristems can be ten times that of other tissues as a result of elevated metabolism and cytoplasmically dense cells (Table 1, Ramakrishnan and Curtis, 1995). Therefore, the local oxygen requirement is not dictated by the average BOD, but the BOD at the meristems. Transport of oxygen is characterized by a flux, and the flux required to support a given rate of respiration is easily calculated from the total respiration within a living tissue, divided by the surface area of the tissue.

$$\text{Flux}\left[\frac{\text{oxygen transport}}{\text{surface area}}\right] = \frac{BOD \cdot FW}{A_{tissue}} \qquad (2)$$

A simple calculation with yeast demonstrates the implications of working with large cell aggregates. Yeast (BOD = 2000 μmol O_2 g^{-1} FW h^{-1}; diameter = 0.01 mm; FW = 2.8×10^{-10} g) will have a surface flux requirement of 0.025 μmol O_2 cm^{-2} h^{-1}. By comparison, an idealized spherical somatic embryo (BOD = 300 μmol O_2 g^{-1} FW h^{-1}; diameter = 1.0 mm; FW = 5.5×10^{-4} g) will have a surface flux requirement of about 5 μmol O_2 cm^{-2} h^{-1}. This shows that even though yeast has a BOD nearly 10 times greater than a plant meristem, the flux requirement at a 1 mm embryo surface could be several hundred times larger than yeast! These calculations not only shed light onto the magnitude of oxygen transfer limitations in plant tissue culture, but also the mechanistic basis of mass transfer. The $k_L a$ of Equation (1) is ubiquitously used in the literature to characterize the transfer of oxygen from the gas to a surrounding liquid medium. The 'k_L' is the liquid-interface mass transfer coefficient, and the 'a' is the bubble interfacial area per unit volume (e.g. Singh and Curtis, 1994). Figure 1 depicts an entirely different mechanism where oxygen transfer is limited by transport at the liquid–solid interface.

This figure shows the two boundary layer mass transfer limitations: the gas–liquid interface adjacent to the bubbles, and the solid–liquid interface adjacent to the plant tissue. The high flux requirement at the tissue surface increases the likelihood that the limiting resistance to mass transfer will be at the plant tissue surface, and not from the gas bubbles. Under these circumstances the oxygen transport rate from the media to the tissue (OTR_{L-S}) becomes:

$$OTR_{L-S} = BOD \cdot \rho_t \cdot V_t = k_{S,required} \cdot A_{tissue}(C_L - C_S) \quad (3)$$

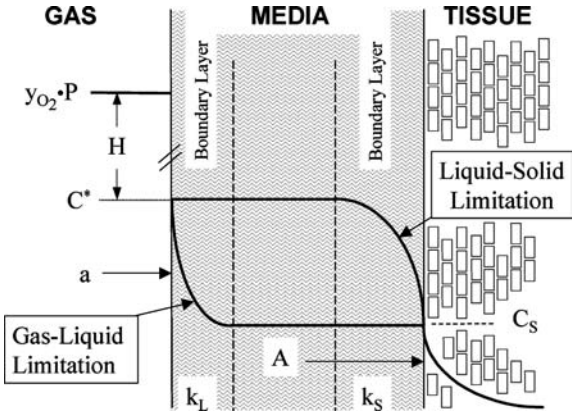

Figure 1. Schematic of gas–liquid and liquid–solid mass transfer resistance. Mass transfer is characterized by mass transfer coefficients at the gas–liquid (k_L) and liquid–solid (k_S) boundary layers. Other parameters are: (y_{O_2}) = mole fraction of oxygen in the gas, (P) = gas pressure, (H) = Henry's law coefficient describing oxygen solubility in water, (a) = interfacial area per unit bioreactor volume, (A) = surface area of tissue, (C^*) = equilibrium dissolved oxygen concentration, (C_L) = liquid dissolved oxygen concentration, (C_S) = dissolved oxygen concentration at the tissue surface.

The surface area of interest now becomes the surface area of the tissue (A_{tissue}), C_S is the dissolved oxygen at the tissue surface, and $k_{S,required}$ is the mass transfer coefficient from the liquid medium to the plant tissue surface that is required to sustain aerobic respiration. Mass transfer coefficients are determined by how fast the media flows past the plant cell aggregate surface (much like the wind-chill factor that determines the rate of heat loss from the skin surface). For a suspended object, the rate of sedimentation provides a reasonable estimate of the velocity that the plant aggregates experience (note that suspended particles will tend to move with the circulation patterns and these bulk flow velocities will not determine the velocity of the embryo relative to its surrounding media). Of particular relevance in this analysis is the suspension of somatic embryos. We have observed that somatic embryo's of oak (*Quercus rubra*) sediment at rates of 1–2 cm s^{-1} for embryo's of 1–2 mm in diameter (Singh and Curtis, 1994) which is consistent with the expected sedimentation rates for dense meristematic tissue. Once a estimate of the velocity is known, there are engineering correlations to calculate the mass transfer coefficient (k_S). For example, the correlation for a sedimenting spherical mass is

$$k_{S,available} = \frac{D_{O_2}}{d_p}\left[2.0 + 0.6\left(\frac{\rho_{media} \cdot v_S \cdot d_p}{\mu_{media}}\right)^{1/2} \times \left(\frac{\mu_{media}}{\rho_{media} \cdot D_{O_2}}\right)^{1/3}\right] \quad (4)$$

This analysis permits a comparison of the mass transfer rates that are 'required' ($k_{S,required}$) by the tissue oxygen demand, and mass transfer rates that

are 'available' due to the flow past the somatic embryo as it is suspended in a bioreactor ($k_{S,available}$). The 'required' oxygen transfer can be calculated using Equation (3) together with approximations for somatic embryo geometry and reasonable assumptions for driving force ($C_L = C^*$; $C_S = C_L/2$). Figure 2 shows the result of this comparison of tissue oxygen need versus oxygen availability.

Calculations are shown for both cylindrical and spherical geometry with similar trends demonstrating that exact details of geometry are not critical. Mass transfer provided in suspension is relatively insensitive to embryo size. In contrast, as the size of the tissue increases, there is a rapid increase in the required oxygen flux and $k_{s,required}$ at the surface. This means that for larger embryos (>1 mm in size), the oxygen demand will exceed availability.

Manipulating oxygen availability

Plant tissues (and embryos in particular) can cope with reduced oxygen availability, therefore it is unclear what the physiological impact would be. None the less, recognizing the physiological changes associated with oxygen availability, it is useful to understand how availability can be controlled in bioreactors. Referring to Equation (3), the only parameter that can be readily manipulated is the liquid dissolved oxygen concentration (C_L). Control of C_L is most easily discussed in terms of the limiting case where the bulk media dissolved oxygen approaches its equilibrium value (C^*) as depicted in Figure 1. The equilibrium dissolved oxygen (D.O.) is dependent on environmental conditions as follows:

$$C_L = C^* = \frac{y_{O_2} \cdot P}{H} \quad (5)$$

It is important to note that equilibrium dissolved oxygen (C^*) is almost never measured; instead, probes are calibrated to give a percentage readout of this complex variable. Each of the parameters of oxygen mole fraction (y_{O_2}), system pressure (P) and Henry's Law coefficient (H) present different approaches to increasing oxygen availability.

Bioreactor pressure will often enhance oxygen availability as an indirect consequence of bioreactor operation. *In situ* sterilizable bioreactors are pressure-rated autoclaves (sterilized at ~18 p.s.i., 120 °C). The typical approach of operating at a head pressure of 5–10 p.s.i. not only reduces contamination risks from leaks, but can nearly double the equilibrium dissolved oxygen (1 atmosphere = 14.7 p.s.i.). In addition, the hydrostatic pressure (ρ_{H_2O}-g-depth) can be a significant contributor to oxygen transfer driving force (1 atmosphere ≈ 33 feet of water). These observations have interesting implications for liquid culture micropropagation. The productivity of a reasonably efficient somatic embryogenic culture can generate large numbers of embryos in bioreactors smaller than 1000 l. Since scale-up would take place in tanks much smaller than traditional fermentation, the depth effect will be minimal. Use of pressurization (beyond autoclave pressures) is usually avoided due to the prohibitive cost of pressure vessels (Curtis, 1999). However, since 'large-scale' micropropagation can be implemented at a small scale, the pressure rating of the vessel (and associated steel costs) will not dominate overall equipment costs, and use of pressure could be economically feasible if it provides a substantial improvement in micropropagule development.

It is also apparent from Equation (5), that an increase in the Henry's law coefficient (H) will reduce the equilibrium dissolved oxygen pressure. Temperature has the greatest influence on H. As the

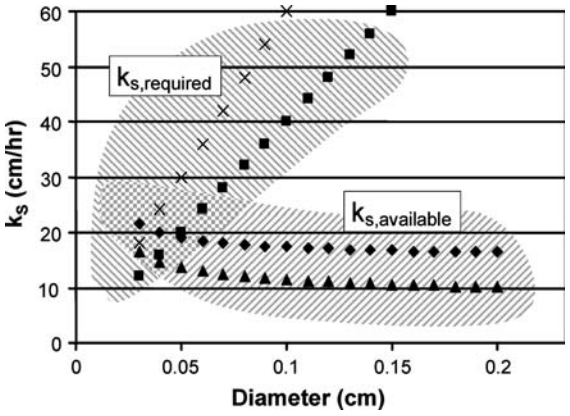

Figure 2. Comparison of oxygen transport required for aerobic respiration and availability in terms of the mass transfer coefficients calculated by Equations (3) and (4). The required mass transfer coefficient ($k_{s,required}$) based on oxygen consumption (BOD = 300 μmol O_2 cm^{-3}(tissue) hr^{-1}) is calculated for cylindrical (×) and spherical (□) plant tissues. The available mass transfer coefficient ($k_{s,available}$) is calculated based on the sedimentation rates that would result for a cylindrical (▲) and a spherical (♦) tissue (ρ_{tissue} = 1.04 g ml^{-1}).

temperature increases, H increases as thermal vibrations exclude oxygen, which decreases the maximum amount of oxygen that can dissolve in the media. Colder temperatures, therefore, favor oxygen solubility (15, 20, 25 and 30 °C correspond to 315, 283, 258, and 236 μmol O_2 respectively in water). To take advantage of the increased oxygen solubility at lower temperatures, an organism must be able to sustain metabolism rates. This is not generally the case for terrestrial plant tissues, therefore, a reduction in temperature will usually significantly reduce the BOD. A suppression of tissue development rates is generally not desirable since it will increase the time-frame required to produce micropropagules. This observation may, however, be useful if it is desirable to maintain aerobic respiration within a tissue by simultaneously reducing oxygen demand and increasing oxygen availability through growth at reduced temperatures. While the temperature dependence of oxygen solubility in water is widely known, the dependence of dissolved oxygen on media components receives less attention. Both the presence of inorganic salts and sugars has predictable effects on oxygen solubility. The approach to quantitatively assessing the impact of media components on solubility is more readily determined from an alternative to H that is referred to as the Bunsen coefficient. The Bunsen coefficient (α) is defined as the volume of oxygen dissolved per volume of media (calculated to a reference state of 0 °C, 1 atmosphere pressure) when contacted with pure oxygen ($y_{O_2} = 1$). The deviation of the Bunsen coefficient from pure water (α_0) can be calculated as the sum of positive and negative contributions of media components (Schumpe et al., 1981):

$$\log\left(\frac{\alpha_0}{\alpha}\right) = \sum_{i=1}^{n}\left(K_{\text{organic}} x_{\text{organic}}\right)_i + \sum_{j=1}^{m}\left(\frac{1}{2}\sum_{k=1}^{w} H_k y_k z_k^2\right)_j (x_j) \quad (6)$$

where K_i and H_i are experimentally determined coefficients for (n) different organic components such as sugar and ions of (m) dissociated salts. These coefficients are multiplied by the respective concentrations (x_i) and also the valence squared in the case of ions. The contribution coefficients for some important plant culture media components are given in Table 2 (panel A). Noting that α is roughly proportional to dissolved oxygen, and $\log(y)$ is positive for $y > 1$, a positive value of K_i or H_i will decrease solubility. Nitrate ions (NO_3^-), therefore, reduce solubility, whereas ammonium (NH_4^+) will increase oxygen solubility. The equilibrium solubility of oxygen in several 'typical' plant culture media is presented as Table 2 (panel B), demonstrating that the presence of nutrients generally suppresses oxygen solubility. This effect is relatively small (fresh MS medium has about 4% reduction), but the practice of utilizing high medium osmoticum (e.g. 5× sucrose) to 'harden' somatic embryos in preparation for transfer out of tissue culture conditions can result in a significantly reduced oxygen solubility. The Bunsen coefficient (and its counterpart the Henry's law coefficient) provides a means of quantitatively understanding the dissolved oxygen available to the micropropagule.

Table 2. Influence of media components on media dissolved oxygen

Panel A: Bunsen coefficient contributions (Schumpe et al., 1981)

	K_i/H_i (l mol^{-1})
Sucrose	44
Glucose	8.8
NH_4^+	6.3
NO_3^-	6.2
K^+	5.0
$H_2PO_4^-$	4.5

Panel B: Calculated equilibrium dissolved oxygen in plant culture media (Equation (8))

	O_2 at 25 °C (mg l^{-1})
Water	8.24
MS (30 g sucrose l^{-1})	7.92
DCR (20 g sucrose l^{-1})	8.04
B5 (20 g sucrose l^{-1})	8.01

MS – Murashige and Skoog, 1962; DCR – Gupta and Durzan, 1985; B5 – Gamborg et al., 1968.

The final and most obvious means of changing the equilibrium dissolved oxygen level is the alteration of the gas oxygen mole fraction. It should be noted that gas composition is altered by water vapor pressure (e.g. 31% reduction in dissolved oxygen for water saturated air at 25 °C. Air is composed of roughly 21% oxygen, and supplementation of plant tissue culture gas with up to 50–60% oxygen is not usually inhibitory for plant tissues. Part of the reason for the lack of toxicity at even higher oxygen levels, is that the tissue does

not actually experience these levels of oxygen since there is a drop in oxygen to the surface of the tissue due to external mass transfer, and a reduction in oxygen within the tissue due to consumption and limitations in diffusional mass transfer. Oxygen supplementation is not a panacea for increasing O_2 availability. Oxygen supplementation can be quite costly – particularly for the long culture times required for plant tissue culture. Advances in pressure swing adsorption (PSA) now provide a relatively inexpensive means of oxygen supplementation to a process of the scale under discussion for commercial micropropagation.

Another processing approach for oxygen supplementation worth noting is the separate sparging of high-purity oxygen in very small bubbles. The advantage of this approach is that the driving force for transport from these bubbles will be five times greater than ambient air, and much higher than would be accomplished if the oxygen was mixed with air sparging. The production of small bubbles is useful since the small radius of curvature will create bubbles with high internal pressure that are not prone to coalescence with the sparged air bubbles. Therefore, separate sparging and small gas bubbles avoid dilution of the driving force for oxygen transfer that results when oxygen is mixed with air. The relatively small scale of micropropagation (relative to industrial fermentation) tends to reduce the impact of costs for oxygen supplementation.

Circulation and micropropagule suspension

The relatively rapid sedimentation velocity of plant tissues results in a need for adequate circulation to provide suspension. The sedimentation rate of a nearly spherical object can be estimated from Stokes law,

$$v_{\text{sediment}} = \frac{(\rho_{\text{tissue}} - \rho_{\text{media}})g \cdot d_{\text{p}}^2}{18 \cdot \mu_{\text{media}}} \qquad (7)$$

however, the sedimentation rate is often sufficiently fast that the laminar flow assumptions for this equation are no longer valid and a more involved calculation using a (laminar–turbulent) drag coefficient is needed (Singh and Curtis, 1994). This equation, none the less, provides the important functional dependencies. The density of the media (ρ_{media}) is roughly the density of water, therefore, the more dense the tissues, the faster they will sediment. We observed the sedimentation rate of oak embryos to correspond to a tissue density of about 1.05 g ml^{-1}, which was considerably faster than unorganized plant cell aggregates (Singh and Curtis, 1994). Gravity (g) is a constant, and the effective viscosity of the media (μ_{media}) will increase when there are more cells present in the suspension, or if the suspended plant tissues are elongated (Curtis and Emery, 1993). The diameter of the suspending particle (d_{p}) is important for this analysis because it has a square dependence – and because plant micropropagules such as somatic embryos are extremely large by comparison to 'typical' microbial suspensions. For example, a suspension of embryos could be expected to sediment a 1 cm in a non-agitated culture flask in about 1 s. By comparison, a yeast suspension would require about 1 h to sediment over the same depth. Preventing sedimentation of plant tissues to the bottom of a bioreactor can become a problem due to their rapid sedimentation rate and the relatively low energy inputs typically used for growth of plant tissues in bioreactors.

To study the issue of somatic embryo suspension more thoroughly, two ~30-l vessels were

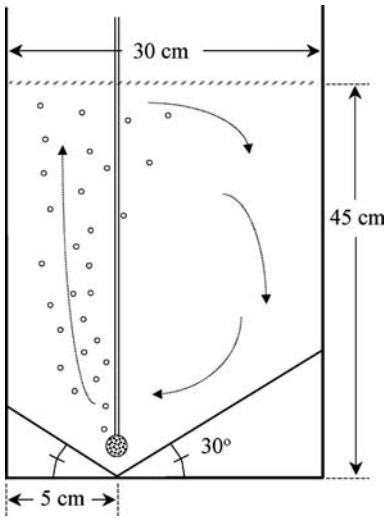

Figure 3. Schematic of the internal loop air-lift bioreactor used to study suspension and mixing intensity. The air-lift exterior is a glass tank with bottom baffling constructed of plexiglass (poly-methyl methacrylate) and sealed in place with silicone glue. Sparging was through two 0.2 μm HPLC mobile-phase spargers (Supelco, Bellfonte, PA). Off-center sparging and baffling geometry was based on previous studies to achieve high mixing with low gas flow rate.

constructed. Polystyrene beads ($\rho = 1.05$ g ml^{-1}) with a diameter of 3.2 mm ($v_{\text{sediment}} = 5.1$ cm s^{-1}) were used to represent somatic embryos in these suspension studies. The first 'bioreactor' used only gas sparging and had a geometrical design based on a recent low-cost bioreactor patent (Curtis, 2001) and is shown schematically in Figure 3.

The large glass tank had a 30° off-center baffling to facilitate circulation at minimum gas flow rates. Sparging was accomplished with dual sintered metal spargers parallel to the baffle vertex. The medium was water containing 4 g l^{-1} NaCl to provide for an ionic strength similar to plant culture medium so that bubble formation and coalescence would provide circulation patterns analogous to a plant cell culture bioreactor. A gas flow rate in this system of 1.4 l min^{-1} (or approximately 0.05 vvm; volume of gas per volume of liquid per minute) provided good circulation rates, but was inadequate to suspend the polystyrene beads. Full suspension was not achieved until approximately 0.12 vvm. This shows that suspension can be achieved at a reasonable gas flow rate with proper design. The loop-configuration for an air-lift bioreactor is particularly good for suspensions because the suspensions' requirements can be met by achieving a riser (bubble upflow region) velocity greater than the sedimentation velocity of the particles. It should be noted that simple sparging in a tank without proper design would invariably result in regions with poor circulation which would accumulate unsuspended tissue and subject it to oxygen deprivation. A qualitative observation based on other unpublished studies, is that achieving suspension in small bioreactors (1–5 l) can be more problematic than larger bioreactors (25–150 l) at comparable gassing rates. The second tank was implemented as a stirred tank using a 6-in. marine propeller and rpm tachometer. The polystyrene beads could be suspended off the bottom at 300 rpm, but uniform suspension required 350 rpm. This is a much higher rpm than typically used for plant cell suspensions at this scale, and the resulting tip speed ($\pi N \cdot D_{\text{impeller}}$) of 280 cm s^{-1} is nearly 5-times greater than our typical starting point of 50 cm s^{-1} used for plant cell suspension culture (Curtis and Singh, 1994). As will be discussed in more detail in the next section, the power level in the stirred tank is much higher than a well-designed air-lift. The chaotic flow patterns in a stirred tank will result in upward flows enhancing suspension, as well as downward flows that aid sedimentation.

Mixing, 'shear' and turbulence

Mixing is fundamentally different from circulation. Mixing is the dispersion of a fluid element throughout the bioreactor, while circulation is the movement of that fluid element to a different location. Mixing can be evaluated either at the scale of total bioreactor volume, or with respect to the small flow patterns that ultimately dissipate the flow energy to thermal energy. It is these small-scale 'eddies' that are often discussed in terms of fluid-dynamic damage to suspended cells. The size of the smallest flow eddies can be characterized by a turbulence length scale referred to as the Kalmogorov length scale (λ_K). This can be estimated from the rate of power dissipation per unit mass of media in the bioreactor ($\hat{P}\rho_{\text{media}}$).

$$\lambda_K = \left(\frac{(\mu_{\text{media}}/\rho_{\text{media}})^3}{\hat{P}/\rho_{\text{media}}} \right)^{1/4} \tag{8}$$

For mechanical agitation, $\hat{P}$ can be calculated based on the impeller speed (N), impeller diameter (D_{impeller}) and a 'impeller power number' that depends on the impeller geometry.

$$\hat{P}_N = \frac{\rho_{\text{media}} \cdot N_P \cdot N^3 \cdot \left(D_{\text{impeller}}\right)^5}{V_{\text{media}}} \tag{9}$$

The power input for gas sparging can be estimated assuming isothermal ideal gas expansion of the sparged gas over the unaerated tank height (h_0).

$$\hat{P}_g = \frac{Q_{\text{top}} P_{\text{top}}}{V_{\text{media}}} \ln\left(\frac{P_{\text{top}} + \rho_{\text{media}} \cdot g \cdot h_0}{P_{\text{top}}} \right) \tag{10}$$

Note that it is necessary to specify the gas flow at the top of the tank (Q_{top}) as well as the pressure at the surface of the media (P_{top}) since both pressure and gas flow rate change throughout the depth of a tank.

The studies of polystyrene bead suspension provided a basis for examining the conditions required for growth of somatic embryos. The air-lift system required a gas flow of 3.6 l min^{-1} sparging into 28 l of liquid with an unaerated liquid height of 45 cm. The resulting power dissipation rate (Equation (10)) is approximately 0.01 W l^{-1} giving a Kalmogarov eddy length of 98 μm. Suspension in the agitated tank ($V_{\text{media}} = 38$ l, $N_{\text{p}} = 0.5$, $N = 300$–350 rpm)

occurred at a power level of 0.13-0.21 Watts l^{-1}. This increased energy dissipation rate results in a reduced eddy length of 45–50 μm. The significance of these calculations is depicted in Figure 4.

The eddy length for energy dissipation is a fraction of the size of a typical somatic embryo (Figure 4a). This means that the plant tissue will experience large variations in local flow velocity from these turbulent eddies. This phenomenon is qualitatively the basis of fluid shear stress on suspended tissues. Figure 4b shows the analogous scenario for a yeast fermentation taking place in a high-intensity stirred tank fermentation at 2–4 W l^{-1}. Despite increasing power levels by 1–2 orders of magnitude, the eddy lengths are still several times larger than the diameter of yeast. As a result, yeast will move with eddies and not 'feel' the fluid shear experienced by larger plant tissue aggregates. It is important to keep in mind that the size of plant micropropagules alters the interpretation of 'low shear' growth conditions.

It is tempting to think of suspensions of cells as a homogeneous fluid, which is implied by discussion of fluid shear and stress. This is a reasonable assumption for microscopic cell suspensions, but this is not the case for suspensions of aggregates that have significant mass and differential density. It is extremely difficult rigorously to characterize flow of an inertial suspension, since this would require considerations of hydrodynamic forces on particles and the associated inertial particle acceleration. Approaches to dealing with these problems are still being developed and not within the scope of this discussion. None-the-less, a qualitative observation related to this behavior is relatively easy to understand and shown pictorially in Figure 5.

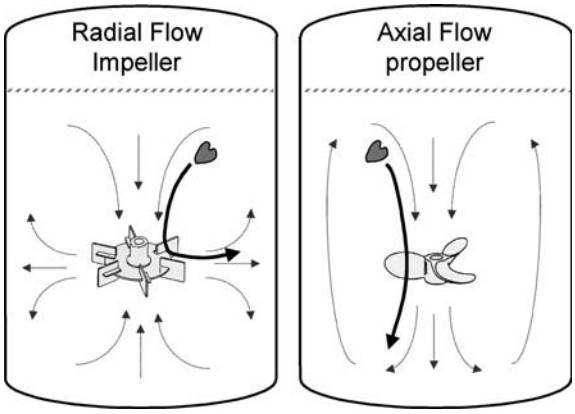

Figure 5. Implications of impeller flow patterns on 'inertial flow' and impeller impact on plant aggregates. Radial flow impellers draw flow inward from above and below with discharge towards the wall. Axial flow propellers push flow along the axis of the impeller shaft. Solid arrow represents typical embryo flow path through the impeller zone.

This figure shows schematics of a stirred tank bioreactor with both axial (marine) and radial (Rushton) flow impellers. In the case of the radial flow impeller, a somatic embryo must dramatically change its flow direction while moving through the impeller zone. In contrast, the embryo can pass through the axial flow impeller zone without changing direction.

The more 'inertial' a particle (larger, more dense), the greater it will resist a change of flow direction. The result is that the particle will be hit by the impeller. This behavior is evident in suspension studies of polystyrene 'embryos'. During suspension with a radial flow impeller, there is a continuous sound of the beads being struck by the impeller. Impeller collisions were reduced

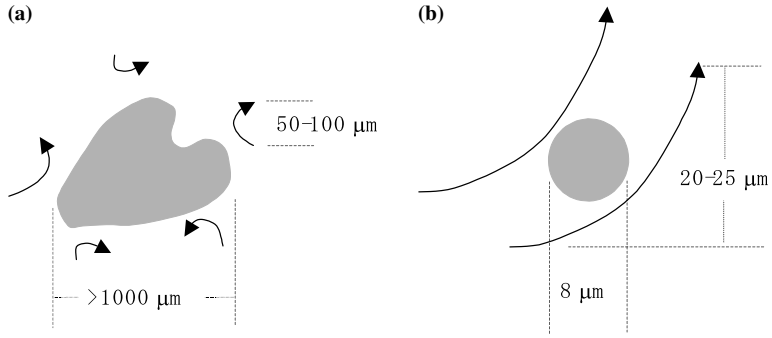

Figure 4. Schematic to depict the microscopic flow patterns calculated as the Kalmogorov eddy length (Equation (8)). For somatic embryos (a) the power level is based on minimum required for suspension of 3.2 mm polystyrene beads in air-lift and stirred tank vessels; for yeast (b) the power level is a typical high-intensity stirred tank fermentation.

significantly at comparable power input levels for the axial flow propeller. It is reasonable to extrapolate from these observations (and this has been experimentally confirmed) that an axial-flow impeller would perform better for aggregated plant cell suspensions. While improved performance might be attributed to 'low-shear' impeller design, the behavior has little to do with fluid shear. This concept shows that it is not necessary to analyze fully the problem to implement a design. In fact, it is possible to implement successfully bioreactors based only on empirical observation of what 'works best'. None-the-less, it is helpful to understand basic principles such as those discussed in this review to help guide the process of design, reduce 'trial-and-error' effort, and better overcome invariable problems that will arise as a system is implemented.

Limitations

It is worth noting that the physiological requirements for plant tissue differentiation may present some incompatibility with traditional concepts inherent in bioreactor design for submerged culture. For example, one premise of suspended liquid systems is that achieving mixing is desirable. However, if embryo development benefits from lack of homogeneity (such as the gradients inherently provided by agar-based culture), then the liquid-suspended system will never provide the desired environmental conditions for embryo development. Under these circumstances, entirely different bioreactor designs should be contemplated. Acknowledging this issue, we implemented a 300 cm^2 inclined plane perfusion bioreactor to provide for the transition from embryogenic carrot cell suspension to fully germinated seedlings by perfusing the system with auxin-free medium (unpublished). A comparable level of normal plant development did not occur in the same time frame for the carrot culture liquid suspension. The wide array of bioreactor designs that are being developed indicates that there will likely be many different 'solutions' that will depend on both the plant tissue being propagated, as well as the scale and economics associated with the particular product. For these different bioreactor configurations, the principles of mixing, oxygen transfer, and biological oxygen demand do not change, however, the details of the analysis and their application can be extremely different. Mathematics is simply a convenient way to express logic; therefore, logic (and common sense) are often the most powerful tools for bioreactor design.

Nomenclature

n number of organic molecules in medium
m number of salts in medium
w number of dissociated ions from a dissolved salt
a interfacial area per unit volume (e.g. $k_L a$), cm^{-1}
A_{tissue} surface area of the tissue, cm^2
BOD biological oxygen demand, μmol O_2 g FW^{-1} h^{-1}
C^* equilibrium medium dissolved oxygen content, μmol O_2 l^{-1}
C_L medium dissolved oxygen content (in bulk liquid), μmol O_2 l^{-1}
C_S medium dissolved oxygen content at tissue surface, μmol O_2 l^{-1}
d_p particle diameter, cm
D_{O_2} diffusion coefficient of oxygen in media, cm^2 s^{-1}
$D_{impeller}$ impeller diameter, cm
FW fresh weight, g
g gravitational acceleration = 980 cm s^{-2}
h_0 height of unaerated liquid in bioreactor, cm
H henry's law coefficient, atm l $(\mu mol\ O_2)^{-1}$
H_k experimental coefficients for the kth dissociated medium ion in Bunsen correlation (Equation (6)), l mol^{-1}
k_L mass transfer coefficient at liquid–gas interface, cm s^{-1}
k_s mass transfer coefficient at solid–liquid interface, cm s^{-1}
$k_{s,available}$ mass transfer coefficient at solid–liquid interface that is available as a result of flow past solid, cm s^{-1}
$k_{s,required}$ mass transfer coefficient at solid–liquid interface that is needed to supply oxygen demand, cm s^{-1}
$K_{organic,i}$ experimental coefficients for the ith organic media component in Bunsen correlation (Equation (6)), l mol^{-1}
N impeller rotational rate, s^{-1}
N_P impeller power number, dimensionless
OTR oxygen transfer rate, μmol O_2 h^{-1}
OTR_{g-L} oxygen transfer rate from the gas to liquid, μmol O_2 h^{-1}
OTR_{L-s} oxygen transfer rate from the liquid to tissue surface, μmol O_2 h^{-1}
OUR oxygen uptake rate (specific), μmol O_2 g FW^{-1} h^{-1}
P local system pressure, atm
P_{top} pressure at the top surface of liquid, atm
$\hat{P}$ power per unit volume, W l^{-1}
$\hat{P}_N$ power per unit volume due to impeller mixing, W l^{-1}
$\hat{P}_g$ power per unit volume due to gas sparging, W l^{-1}
Q_{top} volumetric gas flow rate at top (surface) of bioreactor, cm^3 s^{-1}
v_s, $v_{sediment}$ sedimentation velocity, cm s^{-1}
V_{media} volume of media in bioreactor, cm^3
V_t tissue volume, cm^3
vvm volume of gas sparged per volume of liquid per minute, min^{-1}
x_j concentration of ions in liquid phase, mol l^{-1}
$x_{organic,i}$ concentration of organic components in liquid phase, mol l^{-1}

y_j number of ions of type j in salt
y_{O_2} mole fraction of oxygen in the gas phase, dimensionless
z_{k14} valance of dissociated ion, dimensionless

Greek symbols

α Bunsen coefficient, volume of oxygen dissolved per volume of media at 0 °C and 1 atm, dimensionless
α_0 Bunsen coefficient of pure water, volume of oxygen dissolved per volume of media at 0 °C and 1 atm, dimensionless
λ_k Kalmogorov length scale, cm
μ_{media} viscosity of media, dyne sec cm^{-2} $= g\ cm^{-1}\ s^{-1}$
ρ_{H_2O} density of water, g cm^{-3}
ρ_{media} media density, g cm^{-3}
ρ_t, ρ_{tissue} tissue density, g cm^{-3}

Acknowledgements

I thank Undergraduate Researchers Olatilewa O. Awe and Adam J. Pingel for implementing the polystyrene bead suspension studies in the air-lift and stirred tank bioreactors, respectively. We would like to acknowledge grant support from the National Science Foundation Grants No. BES-0003926, BES-9522033 for support of our research in bioreactor design.

References

Altman PL & Dittmer DS (1968) Metabolism, Biological Handbooks. Federation of American Societies for Experimental Biology, Bethesda, MD

Asplund PA & Curtis WR (2001) Intrinsic oxygen use kinetics of transformed root culture. Biotechnol. Prog. 17: 481–489

Blanch HW & Clark DS (1997) Biochemical Engineering. Marcel Dekker, New York

Curtis WR (1999) Achieving economic feasibility for moderate-value food and flavor additives: a perspective on productivity and proposal for production technology cost reduction. In: Fu TJ, Singh G, Curtis WR (eds) Plant Cell and Tissue Culture for the Production of Food Ingredients (pp. 225–236). Kluwer Academic/Plenum Publishing, New York, NY

Curtis WR (2001) Method and apparatus for aseptic growth or processing of biomass, US Patent # 6,245,555, June 12

Curtis WR & Emery AH (1993) Plant cell suspension culture rheology. Biotechnol. Bioengineering, 42: 520–526

Gamborg OL, Miller RA & Ojima K (1968). Nutrient requirements of suspension cultures of soybean root cells, Exp. Cell Res. 50: 151–158

Gupta PK & Durzan DJ (1985) Shoot multiplication from mature trees of Douglas-fir (*Pseudotsuga menziesii*) and sugar pine (*Pinus lambertiana*). Plant Cell Reports: 177–179

Hsiao TY, Bacani FT, Carvalho EB & Curtis WR (1999) Development of a low capital investment reactor system: application for plant cell suspension culture. Biotechnol. Progr. 15(1): 114–122

Murashige T & Skoog F (1962) A revised medium for rapid growth and bio assays with tobacco tissue cultures. Physiol. Plant. 15: 473–497

Ramakrishnan D & Curtis WR (1995) Elevated meristematic respiration in plant root cultures: implications to reactor design. J. Chem. Eng. Jpn. 28(4): 491–493

Schumpe A, Quicker G & Deckwer WD (1981) Gas solubilities in microbial culture media, In: Feichter A (ed) Advances in Biochemical Engineering, Vol. 24 (pp. 1–38). Springer-Verlag, New York, NY

Singh G & Curtis WR (1994) Reactor design for plant cell suspension culture. In: Shargool PD & Ngo TT (eds) Biotechnological Applications of Plant Culture (pp. 153–184). CRC Press, Boca Raton, FL